JPET Fast Forward. Published on May 31, 2018 as DOI: 10.1124/jpet.118.248427
This article has not been copyedited and formatted. The final version may differ from this version.

Title Page

Ocular Distribution and Pharmacodynamics of SF0166, a Topically Administered $\alpha_v\beta_3$ Integrin Antagonist, for the Treatment of Retinal Diseases

Ben C. Askew, Takeru Furuya, and D. Scott Edwards

SciFluor Life Sciences, Cambridge, MA, USA (BCA, TF, DSE)

JPET Fast Forward. Published on May 31, 2018 as DOI: 10.1124/jpet.118.248427
This article has not been copyedited and formatted. The final version may differ from this version.

Running Title Page

Running title: Ocular Distribution and Pharmacodynamics of SF0166

Corresponding author:

D. Scott Edwards, Ph.D.

SciFluor Life Sciences

300 Technology Square

Cambridge, MA 02139, USA

Phone: 617-684-4752

Fax: 617-684-4758

E-mail: scott.edwards@scifluor.com

No. of text pages: 17

No. of tables: 2

No. of figures: 5

No. of references: 16

No. of words in Abstract: 229

JPET Fast Forward. Published on May 31, 2018 as DOI: 10.1124/jpet.118.248427
This article has not been copyedited and formatted. The final version may differ from this version.

No. of words in Introduction: 428

No. of words in Discussion: 696

Abbreviations: AMD, age-related macular degeneration; ANOVA, analysis of variance; bFGF, basic fibroblast growth factor; BID, twice daily; CAM, chorioallantoic membrane; CnAOEC, canine aortic endothelial cells; CNV, choroidal neovascularization; DME, diabetic macular edema; DR, diabetic retinopathy; HMVEC, human dermal microvascular endothelial cells; HPBCD, hydroxypropyl-beta-cyclodextrin; OCT, ocular coherence tomography; OIR, oxygen-induced retinopathy; OD, left eye; OS, right eye; QD, once daily; PBS, phosphate-buffered saline. PDGF, platelet-derived growth factor; RAEC, rabbit aortic endothelial cells; RLMVEC, rat lung microvascular endothelial cells; VEGF, vascular endothelial growth factor

Recommended section assignment: Drug Discovery and Translational Medicine

Abstract

SF0166, a small molecule $\alpha_v\beta_3$ antagonist, has physiochemical properties that allow distribution to the posterior segment of the eye after topical administration in an ophthalmic solution. The pharmacodynamics and ocular distribution of SF0166 were evaluated in several cell lines, chick chorioallantoic membrane assays, and models of ocular neovascularization in mice and pigmented rabbits. SF0166 inhibited cellular adhesion to vitronectin across human, rat, rabbit, and dog cell lines with IC_{50} values of 7.6 pM to 76 nM. SF0166 inhibited integrin-ligand interactions at IC_{50} values of 0.6 nM to 13 nM for human $\alpha_v\beta_3$, $\alpha_v\beta_6$, and $\alpha_v\beta_8$. SF0166 significantly decreased neovascularization in the oxygen-induced retinopathy mouse model. SF0166 distributed to the choroid and retina after topical ocular administration in amounts that substantially exceeded the cellular IC_{50} for adhesion to vitronectin; drug concentrations were maintained for >12 hours. In the laser-induced choroidal neovascularization model, topical ocular administration of SF0166 decreased lesion area compared with vehicle and was comparable to a bevacizumab injection. In the vascular endothelial growth factor-induced early neovascularization and vascular leakage model, topical ocular application of SF0166 resulted in a dose-dependent reduction in vascular leakage; the highest ocular doses tested showed comparable activity to a bevacizumab injection.

INTRODUCTION

Age-related macular degeneration (AMD) and diabetic retinopathy (DR) are leading causes of visual impairment and blindness worldwide that continue to grow in prevalence as the population ages and the incidence of diabetes mellitus increases (Bourne et al., 2013; Foster and Resnikoff, 2005; Congdon et al., 2004). Intravitreally injected inhibitors targeting vascular endothelial growth factor (VEGF) have had a significant impact on the treatment of neovascular AMD and diabetic macular edema (DME), a manifestation of DR. Antagonists of $\alpha_v\beta_3$ and $\alpha_v\beta_5$ block VEGF-R2 phosphorylation and VEGF-stimulated adhesion, proliferation, and migration of endothelial cells (Tsou and Isik, 2001; Terai et al., 2001). After ocular VEGF exposure in monkeys, $\alpha_v\beta_3$ and $\alpha_v\beta_5$ are up-regulated in migrating cells from pre-existing and newly formed vessels (Witmer et al., 2004). This evidence indicates a relationship between VEGF and α_v integrins and supports the investigation of α_v integrin antagonists to treat neovascular AMD and DME.

Small molecule antagonists of $\alpha_v\beta_3$ and $\alpha_v\beta_5$ have been shown to inhibit retinal neovascularization in animal models when administered by intraperitoneal or periocular injection (Wilkinson-Berka et al., 2006; Luna et al., 1996). JNJ-26076713, when administered orally, has been shown to inhibit retinal neovascularization in an oxygen-induced model of retinopathy of prematurity as well as inhibiting retinal vascular permeability in diabetic rats, a key early event in DME and neovascular AMD (Santulli et al., 2008).

AXT107, a 20-mer peptide that binds to $\alpha_v\beta_3$ and $\alpha_5\beta_1$, has recently been reported to suppress sub-retinal and retinal neovascularization in two mouse models after intra-ocular injection (Silva et al., 2017). In a rabbit model, injection of AXT107 significantly reduced VEGF-induced vascular leakage comparable to an injection of aflibercept but showed a longer duration of action after a single injection.

ALG-1001 (Luminate®) is reported to be a peptide inhibitor of $\alpha_v\beta_3$, $\alpha_v\beta_5$, $\alpha_5\beta_1$, and $\alpha_3\beta_1$ (Kupperman, 2015) and is being studied in clinical trials for the treatment of DME (NCT02348918) and vitreomacular adhesion (NCT02153476), by intravitreal injections.

SF0166 is a potent $\alpha_v\beta_3$ antagonist with appropriate physiochemical properties to allow distribution to the posterior segment of the eye after topical administration in an ophthalmic solution.

Herein, we describe the in vitro anti-adhesion and anti-angiogenic activity of SF0166, efficacy in a mouse model of oxygen-induced retinopathy (OIR), and in vivo ocular distribution and efficacy in Dutch-Belted rabbit models of laser-induced choroidal neovascularization (CNV) and VEGF-induced neovascularization. SF0166 is currently being investigated in 2 clinical trials in patients with DME (NCT02914613) and neovascular AMD (NCT02914639). Successful clinical development would provide a topically applied ocular treatment for DME and neovascular AMD that may replace intravitreal injections of anti-VEGF biologic drugs.

JPET Fast Forward. Published on May 31, 2018 as DOI: 10.1124/jpet.118.248427
This article has not been copyedited and formatted. The final version may differ from this version.

METHODS

Test Materials and Cell Lines

SF0166-FA, (*S*)-3-(6-(difluoromethoxy) pyridin-3-yl)-3-(oxo-2-3-(3-(5,6,7,8-tetrahydro-1,8-naphthyridin-2-yl)propyl)imidazolidin-1-yl)propanoic acid (molecular weight of 475 g/mol), and SF0166, the 2-amino-2-methyl-2-propanol salt (molecular weight of 565 g/mol), was manufactured by Anthem Biosciences (Bangalore, India) (Askew et al., 2014). Both forms of the test article are referred to as SF0166 in this article. The free acid form (SF0166-FA) was used in all studies except the VEGF-induced neovascularization in Dutch-Belted rabbits and the ocular distribution analyses in rabbits.

Human dermal microvascular endothelial cells (HMVEC) were from Lonza (Basel, Switzerland), rabbit aortic endothelial cells (RAEC) were from Cell Biologics (Chicago, IL, USA), rat lung microvascular endothelial cells (RLMVEC) were from Vec Technologies (Rensselear, NY, USA), K562 (leukemia) and HT29 (adenocarcinoma) were from ATCC (Manassas, VA, USA), and canine aortic endothelial cells (CnAOEC) were from Cell Applications (San Diego, CA, USA).

Animals

This research was carried out in accordance with the Guide for the Care and Use of Laboratory Animals as adopted and promulgated by the U.S. National Institutes of Health and was approved by the clinical research organization's review board. Female 129SVE newborn mouse pups with mothers were obtained from Charles River

Laboratories (Wilmington, MA). Male naïve Dutch-Belted rabbits weighing approximately 1.5-2.0 kg were obtained from Covance (Denver, PA) or Western Oregon Rabbit Company (Philomath, OR). Food and water were suppled ad libitum.

Determination of Physiochemical Properties

A 2-phase system plate was used for octanol/buffer partitioning to determine Log D values. Octanol in equilibrium with universal buffer (0.15 M NaCl and 0.100 M each of phosphoric, boric, and acetic acids) adjusted with NaOH to pH 2.0, 4.0, 7.4, and 9.0. SF0166 and standards in 10 mM DMSO were added to the plates for a final concentration of 10% DMSO. The plates were sealed, vortexed, and centrifuged to aid in phase settling. The assay was conducted on a ADW workstation using chemiluminescent nitrogen detection (Analiza, Cleveland, OH). Calculated log D values were corrected for background nitrogen.

To determine pKa values, SF0166 in 10 mM DMSO was diluted with 2 mM HCl and methanol to achieve final concentrations of 60% methanol, 100 µM SF0166, and 1% DMSO. The assay was conducted in 96-well plates using a pKa PRO Analyzer and Estimator software (AATI, Ames, IA). The average pH spacing between buffer points was 0.4 pH units, covering a pH range of 1.7 to 11.2. Four consecutive runs were conducted starting with 60% co-solvent and decreasing to 30% co-solvent buffers.

To assess permeability, SF0166 in 10 mM DMSO was diluted with 1x PBS for a final concentration of 200 µM SF0166 and loaded onto a BD Gentest Pre-coated PAMPA plate (BD Biosciences, San Jose, CA) and incubated 5 hours in the dark at ambient temperature. Samples were then diluted 20-fold with a 50:50 mixture of mixture of

mobile phase components (0.1% formic acid in water:0.1% formic acid in acetonitrile) and analyzed using an Agilent Technologies (Santa Clara, CA) 1100 HPLC coupled with a CTC HTC-PAL autosampler (CTC Analytics, Lake Elmo, MN) and AQUASIL C18 column (3 µM, 50 x 2.1 mm; Thermo Fisher Scientific, Waltham, MA). TOF-MS data were acquired using an Agilent 6538 Ultra High Accuracy TOF MS in extended dynamic range (m/z 100-1000) using generic MS conditions. Following data acquisition, exact mass extraction and peak integration were performed using MassHunter Software (Agilent Technologies).

Binding to $\alpha_v\beta_3$, $\alpha_v\beta_5$, $\alpha_v\beta_6$, and $\alpha_v\beta_8$ Integrins

SF0166 was assessed for binding to $\alpha_v\beta_3$, $\alpha_v\beta_5$, $\alpha_v\beta_6$, and $\alpha_v\beta_8$ integrins using a previously published in vitro assay (Ludbrook et al., 2003). Briefly, $\alpha_v\beta_3$, $\alpha_v\beta_5$, $\alpha_v\beta_6$, and $\alpha_v\beta_8$ integrins (R&D Systems; Minneapolis, MN) were coupled to Dynabeads M-270 Epoxy (ThermoFisher Scientific, Waltham, MA), and conditions for the binding of the coupled Dyna beads to the integrins' respective ligands were optimized. Ligands were as follows: vitronectin (R&D Systems) for $\alpha_v\beta_3$ and $\alpha_v\beta_5$; LAP TGF-β1 (R&D Systems) for $\alpha_v\beta_6$ and $\alpha_v\beta_8$. Each integrin-ligand pair was treated with SF0166 at concentrations of 3.9-500 nM in 0.08% DMSO (triplicate measures). After a 3-hour incubation, the beads were washed, labeled with a primary antibody to the ligand (R&D Systems) and a secondary antibody conjugated with FITC (Sigma), and analyzed by flow cytometry. The method was validated by screening the effect of echistatin, cilengitide, and CWHM12 (synthesized by Anthem BioSciences, Bangalore, India; Henderson et al., 2013) on the appropriate integrin-ligand pair. IC_{50} values were determined using Prism software (GraphPad, La Jolla, CA).

Testing of Anti-Adhesion Activity

The activity of SF0166 in blocking adhesion to vitronectin was assessed in HMVEC, RAEC, and RLMVEC and in blocking adhesion to vitronectin and fibronectin was assessed in CnAOEC. (Adhesion to vitronectin is mediated by $\alpha_v\beta_3$ and $\alpha_v\beta_5$; adhesion to fibronectin is predominantly mediated by $\alpha_5\beta_1$.)

HMVEC cells were used at passages 9-14, and RAEC and RLMVEC cells were used at passages 4-14. Cells were grown in T175 tissue culture flasks and dislodged by gentle 3 min treatment with Accutase. After washing, the cells in suspension in RPMI were loaded with calcein-AM (5 µM) for 30 min at 37°C and re-suspended into RPMI without phenol red containing 10% FBS. Assays were performed in 96-well plates, which were coated with vitronectin in PBS, pH 7.4, by incubating 50 µL of 10 µg/mL solution for 1.5 h at room temperature or overnight at 4°C. The plates were then blocked with 1% BSA in PBS (30 min at room temperature) and washed with PBS. Cell suspensions were plated at a density of 5.0×10^4 (HMVEC and RAEC) or 1.0×10^5 (RLMVEC). SF0166 was added at the same time as the cells. Two lots of SF0166 were tested. The compound was tested using a maximum concentration of 1 µM with half-log dilutions. The plates were incubated for 1.5 h at 37°C. The plates were gently washed with 2 cycles of aspiration of the supernatant and addition of 100 µL of pre-warmed fresh DPBS.

CnAOEC were used at passages 4-6. Cells were grown in T75 or T175 tissue culture flasks in Canine Endothelial Cell Growth Medium (Cell Applications); cells were then washed with DPBS containing 0.5M EDTA, then incubated 5-10 min with enzyme-free

cell dissociation solution (Sigma). After washing, the cells were diluted to 400 cells/µL in Canine Endothelial Cell Growth Medium. Assays were performed in 96-well plates, which were coated with vitronectin (50 µL of 10 µg/mL solution; 500 ng/well) or fibronectin (1 µg/mL; 50 ng/well) in DPBS by incubating for 2 h at room temperature. The plates were then blocked with 1% BSA in PBS (30 min at room temperature) and washed with PBS. SF0166 was tested using a maximum concentration of 1 µM with half-log dilutions. After addition of SF0166, cell suspensions were added at a density of 2.0×10^4 cells/well. The plates were incubated for 1 h at 37°C. The plates were gently washed with 2 cycles of aspiration of the supernatant and addition of 100 µL of pre-warmed fresh Canine Endothelial Cell Growth Medium. An equal volume of Alamar Blue (0.1 mM resazurin solution in DPBS) was added to each well and incubated for 1 h at 37°C.

The activity of SF0166 was compared with L-000845704 (Murphy et al., 2005), a positive control, for inhibiting the binding to vitronectin and fibronectin of HMVE, RLMVEC, K562 (leukemia), and HT29 (adenocarcinoma) cell lines. HMVEC cells were used at passages 9-14, RLMVEC and HT29 cells were used at passages 4-10, and K562 cells were used at passages 3-8. Cell culture and assays were conducted as described above with the following differences. Cell suspensions were plated at a density of 2.0×10^5. SF0166 was tested at 10 concentrations with a half-log dilution schedule. Cell adhesion to vitronectin was tested in duplicate or triplicate at compound concentrations ranging from 316 nM to 0.317 pM. Cell adhesion to fibronectin was tested in duplicate or triplicate at compound concentrations ranging from 200 µM to 20 nM for HMVEC and K562 cell lines and from 316 nM to 0.317 pM for HT29. The

plates were gently washed with 1 cycle of aspiration of the supernatant and addition of 100 µL of pre-warmed fresh DPBS.

Fluorescence of adherent cells was measured using a multimode plate reader (Victor 2V, PerkinElmer, Waltham, MA) at excitation/emission wavelengths of 485/535 nm. IC_{50} values were calculated with Prism software by fixing the bottom of the curves to a value of blank for empty wells.

Anti-angiogenic Activity Using Chick Chorioallantoic Membrane (CAM) Assay – bFGF-, VEGF-, and PDGF-Induced Models

The ovo anti-angiogenic activity of SF0166 was assessed using the CAM model, a model of angiogenesis that is widely used for evaluation of anti-angiogenic therapies (Ponce and Kleinman, 2003). Fertile hen eggs were procured from a hatchery and were cleaned and decontaminated with alcohol. One milliliter of albumin was removed by syringe and incubated for 8 days. CAM surfaces were grafted with gelatin sponges impregnated with 0.5-5 µg of SF0166, dissolved in PBS along with 50 ng of basic fibroblast growth factor (bFGF), VEGF, or platelet-derived growth factor (PDGF). Staurosporine 1 µg was used as a positive control. The CAMs were further incubated to Day 12, and on Day 12 the CAMs were fixed with 4% formaldehyde in PBS, dissected, and imaged. Imaging was performed under constant illumination and magnification using a stereo microscope fitted with a digital camera. Image analysis was performed by drawing a ring around each graft and counting the number of vessels crossing the ring (blood vessel score). Data were analyzed using Excel 2007.

Ocular Distribution

The ocular uptake and ocular tissue distribution of SF0166 was assessed after a single topical ocular administration into both eyes in Dutch-Belted rabbits. The vehicle was boric acid, hydroxypropyl-beta-cyclodextrin (HPBCD), EDTA, and benzalkonium chloride. SF0166 was administered at a concentration of 5% and a volume of 50 µL/eye (2.5 mg/eye). Plasma and the ocular tissue samples (aqueous humor, vitreous humor, sclera, and retina-choroid-plexus) were collected at 1, 4, 8, and 12 hours post dose (n = 3 animals [6 eyes] per timepoint) and stored frozen until analysis. Working solutions were prepared in 50:50 acetonitrile:water. Working solutions were combined with plasma, a 1:1 mixture of aqueous and vitreous humor, or a mixture of blank homogenized sclera, retina, and choroid to make 8-point calibration curves. Plasma samples were analyzed using a validated LC-MS-MS procedure. Briefly, 100 µL aliquots were mixed with 0.75 mL acetonitrile (Spectrum, New Brunswick, NJ) containing 10 ng of SF0166-*d3* internal standard. After shaking for 5 minutes, the sample was centrifuged to remove precipitated proteins, and 200 µL of the resulting supernatant was transferred to an autosampler tube, diluted with 0.5 mL of ASTM Type I water, and vortex-mixed for instrumental analysis. For the determination of SF0166 in vitreous and aqueous humor, study specimens were homogenized in a shaker for 1 hour, centrifuged, and aliquots taken for extraction and analysis. Ocular tissue specimens were finely cut, weighed, and treated with 30 parts (extraction volume [µL] to sample weight [mg]; 3 parts for lens tissue) of ASTM Type I water and shaken for approximately 0.5 hour. Sample extraction was repeated after the addition of 10 parts of ACN (1 part for lens tissue) and another 0.5 hour of shaking. The samples were then

centrifuged, and aliquots taken for extraction and analysis. The specimen aliquots (100 µL) were treated with 200 µL of ACN containing internal standard and shaken for approximately 0.5 hour. The samples were then centrifuged to remove precipitated proteins and diluted with 200 µL of water for instrumental analysis. Samples were analyzed using LC-MS-MS. Ocular pharmacokinetic parameters were determined by noncompartmental analysis using R (version 3.3.1) with the package PKNCA.

OIR Mouse Model

The efficacy of SF0166 was evaluated in the OIR mouse model. On postnatal Day 7, mice were subjected to hyperoxia (75% oxygen) to inhibit retinal vessel growth and induce retinal vessel loss (vaso-obliteration). At postnatal Day 12, mice were returned to a normoxic environment to induce retinal neovascularization. On postnatal Days 13-17, mice received bilateral topical instillation of vehicle or 5% SF0166 twice daily (BID). At postnatal Day 18, retinal tissue was collected, processed, and analyzed to measure vaso-obliteration and neovascularization.

Retinas were stained with isolectin B4 to selectively label retinal vasculature. Stained retinal flat-mounts were imaged and analyzed to quantify both vaso-obliteration, defined as the avascular area central to the optic nerve, and neovascularization. Statistical analyses were performed using Prism software using an unpaired t-test.

Laser-Induced CNV Model in Dutch-Belted Rabbits

In the laser-induced CNV model, the safety and efficacy of SF0166 were evaluated over 5 weeks using clinical ophthalmic exams, ocular coherence tomography (OCT), fundus

photography, and fluorescein angiography. Prior to placement on study, animals underwent pre-screening ophthalmic examinations, including slit-lamp biomicroscopy and indirect ophthalmoscopy. Ocular findings were scored as shown in Supplemental Table 1. Only animals with a score of 0 in all categories were included in the study. Animals were anesthetized for CNV induction and one drop of topical proparacaine hydrochloride anesthetic (0.5%) was placed in each eye before procedures. CNV was induced by laser treatment on Day -3. An external diode laser was applied to the retina using a laser contact lens and a slit-lamp biomicroscope. Both eyes of each animal underwent laser photocoagulation treatment (18-23 spots per eye sized 20-100 µm). Following laser treatment, 50 µL of a 25 µg/mL VEGF solution (1.25 µg dose) was injected intravitreally into each eye, which prolongs the viability of CNV induced by laser injury (Gum et al., 2005). Topical antibiotic ointment was applied after the laser CNV induction procedure. Overall safety was assessed through daily general health and gross ocular observations.

The test articles were SF0166, bevacizumab (Avastin®) as positive control, and vehicle. The SF0166 consisted of 2.5 wt% SF0166 dissolved in PBS containing 5 wt% sulfobutyl ether beta-cyclodextrin. SF0166 (1.25 mg/eye) and vehicle control were administered topically in 50 µL into each eye BID starting on Day 1, except on Day 35 when the terminal ocular distribution study was performed. Bevacizumab (1.25 mg/eye) was administered by intravitreal injection once on Day 1.

The Heidelberg Spectralis OCT (Software version 5.4) was used to capture both the OCT and fluorescein angiography images during the study. Lesion dimensions (widths and heights measured in micrometers) were measured using the OCT images and

utilizing the algorithms of the Heidelberg Spectralis OCT software. Lesion sites that were more uniform in shape and away from any anomalies associated with the initial CNV induction were selected for measurements. Four sites were chosen for each eye, and the same 4 sites were assessed at each timepoint.

The areas of the previously measured lesions were analyzed by individually tracing the overall perimeter of the CNV anomaly using the algorithms of the Heidelberg Spectralis OCT software. Statistical analysis was performed on the area of the lesions for each eye over the course of the study and the data were analyzed using analysis of variance (ANOVA). Differences among groups were analyzed using Dunnett's multiple comparison procedure.

VEGF-Induced Neovascularization Model in Dutch-Belted Rabbits

The VEGF-induced neovascularization and vascular leakage model study evaluated the safety, efficacy, and distribution of SF0166. Prior to placement on study, each animal underwent an ophthalmic examination (slit-lamp biomicroscopy and indirect ophthalmoscopy). Ocular findings were scored as shown in Supplemental Table 2. The acceptance criteria for placement on study were scores of 0 for all variables. Neovascularization and vascular leakage was evaluated by fluorescein angiography and the images were graded to determine the fluorescein angiography score.

Test article administration to the eyes of 6 Dutch-Belted rabbits per group began on Day 1 of the study (2 days prior to VEGF injection [vascular leakage/neovascularization induction]). SF0166 was dissolved in 5% hydroxypropyl beta-cyclodextrin and polyethylene glycol 6000 in borate buffer. SF0166 at concentrations of 1% to 5% (0.5 to

JPET Fast Forward. Published on May 31, 2018 as DOI: 10.1124/jpet.118.248427
This article has not been copyedited and formatted. The final version may differ from this version.

2.5 mg/eye) and vehicle control were administered topically in 50 µL to each eye once daily (QD) or BID as shown in Supplemental Table 3. Bevacizumab (1.25 mg/eye) was administered by intravitreal injection once on Day 1.

Vascular leakage was induced on Day 3 via intravitreal injection of VEGF (500 ng/eye). Clinical ophthalmic examinations and fluorescein imaging were performed at baseline (Day -2) prior to the initiation of dosing and prior to termination on Day 8. Body weights were recorded prior to the start of dosing and prior to termination. Overall safety was assessed through daily general health observations.

The fluorescein angiography images were evaluated according to the scale shown in Supplemental Table 2 to provide a mean fluorescein angiography score.

RESULTS

Physiochemical Properties

SF0166 is an anionic molecule, marginally more lipophilic than hydrophilic, with a high membrane permeability. SF0166 has physiochemical properties as follows: log D (corrected) of -0.13 at pH 2.0; 0.62 at pH 4.0, 0.43 at pH 7.4, 0.01 at pH 9.0; pKa of 4.24 and 7.71; and permeability of 7.72×10^{-7} cm/sec.

In Vitro Studies

SF0166 inhibited human integrin-ligand interactions at IC_{50} values of 0.6 nM for $\alpha_v\beta_3$, 8 nM for $\alpha_v\beta_6$, and 13 nM for $\alpha_v\beta_8$. SF0166 did not inhibit binding to $\alpha_v\beta_5$. The IC_{50} values for inhibition of cell adhesion to vitronectin were 59 nM for human (HMVEC), 76 nM for dog (CnAOEC), 49 nM for rabbit (RAEC), and 7.8 nM for rat (RLMVEC). The IC_{50} values for inhibition of cell adhesion to fibronectin were >1.0 µM for dog (CnAOEC). SF0166 and L-000845704 (positive control) were both potent inhibitors of cell adhesion to vitronectin, with IC_{50} values from 7.6 pM to 1.6 nM (SF0166) and 29 pM to 1.6 nM (L-000845704), depending on the cell line (Table 1). Both were substantially less potent in blocking the cell adhesion to fibronectin, with IC_{50} values of 1.3 nM to 930 µM (SF0166) and 5.3 nM to 239 µM (L-000845704).

In the CAM assay, angiogenesis stimulated by basic fibroblast growth factor (bFGF) was inhibited in a dose-dependent manner, with a 36% reduction in vessel score at 0.5 µg, 42% at 1 µg, and 58% at 4 µg compared with 67% for 1 µg staurosporine, a pan-kinase inhibitor used as the positive control (Fig. 1A). Angiogenesis stimulated by VEGF

JPET Fast Forward. Published on May 31, 2018 as DOI: 10.1124/jpet.118.248427
This article has not been copyedited and formatted. The final version may differ from this version.

was inhibited in a potent dose-dependent manner, with a 61% reduction in vessel score at 2 µg and 88% at 5 µg compared with 90% for 1 µg staurosporine (Fig. 1B). Angiogenesis stimulated by platelet-derived growth factor (PDGF) was moderately inhibited, with a moderate 35% reduction in vessel score at 0.5 µg, 28% at 1 µg, and 28% at 4 µg with no clear dose response. Inhibition with 1 µg staurosporine was 49% (Fig. 1C).

Ocular Distribution

After a single ocular dose, rapid exposure to SF0166 was evident in all rabbits as indicated by plasma and ocular tissue (sclera, retina-choroid, vitreous humor, and aqueous humor) C_{max} values at 1 hour post-dose (the first sampling timepoint) for most tissues (Fig. 2). Ocular tissue pharmacokinetic parameters are shown in Table 2. The concentration of SF0166 in the retina-choroid peaks at 5103 ng/g or 9.0 nmol/g (formula weight of SF0166 is 565 g/mol), or ~9 µM (assuming a tissue density of 1 g/mL).

OIR Model

An increase in vaso-obliteration was seen in the group of mice treated with 5% SF0166 relative to the vehicle treated group, but the difference was not significant (p=0.1412). A significant decrease in neovascularization was observed in the 5% SF0166 treatment group relative to the vehicle treatment group (Fig. 3; p=0.0363).

Laser-Induced CNV Model

There were no notable abnormalities in daily general health and gross ocular observations.

Clinical Ophthalmic Examinations: On Day 0, 3 days after laser treatment and the day before initiation of dosing with SF0166, vehicle, or bevacizumab, animals across groups had scores of 1 or 2 for choroidal/retinal inflammation, retinal hemorrhage, retinal detachments, and vitreal hemorrhage.

Animals treated with SF0166 did not demonstrate any sign of ophthalmic toxicity that was not also present at the same or higher frequency in animals treated with bevacizumab or vehicle. On Day 35 (treatment with SF0166 or vehicle for 34 days), all scores were 0-1 on all measures except lens (score of 3 for all animals except 1 animal in the SF0166 group). Scores of 1 were reported in all groups for cornea and surface area of cornea involvement, retinal detachments, and retinal hemorrhage. Small particles were still present on the posterior capsule of the lens for most animals in all dose groups.

CNV Lesion Area Measurements: Lesion area in the left eye (OD) decreased significantly in the SF0166 group compared with the vehicle control group from Day 4 to the end of the study, and in the bevacizumab group from Day 18 to the end of the study (Fig. 4A). (Comparison between the SF0166 and bevacizumab groups was not attempted since the starting [Day -1] lesion areas were greater for the bevacizumab group [OD and right eye (OS)].) The SF0166 group showed the most decrease in CNV lesion area OS, decreasing significantly compared with the vehicle control group from Day 18 to the end of the study (Fig. 4B).

VEGF-Induced Neovascularization Model

There were no notable abnormalities in daily general health observations.

Clinical Ophthalmic Examinations: Observations at the clinical ophthalmic examination on Day 8 such as slight opacity of the posterior capsule or lens or of the vitreous humor, small localized retinal detachment, and cataract were all mild and may have been artifacts from intravitreal injections or immune reactions to the VEGF administration.

Fluorescein Imaging: Fluorescein image scoring indicated that the VEGF-induced vascular leakage (vehicle control group) was noticeably attenuated both in the bevacizumab group and in all SF0166-treated groups (Fig. 5). The highest degree of leakage occurred in the vehicle group. There was a dose-dependent decrease in the mean fluorescein angiography scores (attenuation of leakage) for SF0166-treated groups. The lowest mean fluorescein angiography score was in the bevacizumab group; however, the highest SF0166 dose groups showed comparable mean scores to bevacizumab. Representative fluorescein images are provided in Supplemental Fig. 1.

DISCUSSION

This is the first report of the pre-clinical pharmacologic activity of an $\alpha_v\beta_3$ inhibitor administered in an eye-drop formulation. Previous studies of $\alpha_v\beta_3$ inhibitors in retinal disease models have utilized intra-ocular or intraperitoneal injection, or oral dosing. These studies provide validation of inhibiting $\alpha_v\beta_3$ for the treatment of retinal disease such as neovascular AMD and DME. The only $\alpha_v\beta_3$ inhibitor that has been tested in patients is ALG-1001, which must be delivered by intravitreal injection. A topically applied $\alpha_v\beta_3$ inhibitor would potentially eliminate the need for repeated intravitreal injections.

SF0166 is the result of a drug discovery effort to synthesize small molecule $\alpha_v\beta_3$ antagonists having the appropriate physiochemical properties to allow distribution to the posterior segment of the eye after topical administration in an ophthalmic solution. A series of analogs of L-000845704, the small molecule $\alpha_v\beta_3$ antagonist clinically tested as a treatment for osteoporosis (Murphy et al., 2005), with a range of physiochemical properties (e.g., LogP) were synthesized by incorporating one or more fluorine substituents, testing their potency as inhibitors of cellular adhesion to vitronectin, and then advancing the compounds with potency comparable to L-000845704 into in vivo testing of ocular distribution and in models of retinal neovascularization and vascular leakage.

SF0166 inhibits ligand binding to the integrins $\alpha_v\beta_3$, $\alpha_v\beta_6$, and $\alpha_v\beta_8$ with nanomolar activity, but does not inhibit binding to $\alpha_v\beta_5$ or cellular binding to fibronectin via $\alpha_5\beta_1$. This integrin selectivity differs from that reported for the other $\alpha_v\beta_3$ antagonists tested

as potential treatments for retinal diseases. ALG-1001 is reported to inhibit $\alpha_v\beta_3$, $\alpha_v\beta_5$, $\alpha_5\beta_1$, and $\alpha_3\beta_1$ (Kupperman, 2015); while SB-267268 and JNJ-26076713 inhibit $\alpha_v\beta_3$ and $\alpha_v\beta_5$ (Wilkinson-Berka et al., 2006; Santulli et al., 2008), and AXT107 inhibits $\alpha_v\beta_3$ and $\alpha_5\beta_1$ (Silva et al., 2017). Despite the absence of activity against $\alpha_v\beta_5$ and $\alpha_5\beta_1$, SF0166 was effective in models of retinal neovascularization and vascular leakage. The potential implications of the inhibitory activity of SF0166 against $\alpha_v\beta_6$ and $\alpha_v\beta_8$ receptors remain to be determined.

SF0166 distributed to the choroid and retina after topical ocular administration in amounts that substantially exceeded the IC_{50} value for binding to $\alpha_v\beta_3$ and for cellular adhesion to vitronectin, and these high drug concentrations were maintained for more than 12 hours. The high levels of SF0166 in the sclera and low levels in the vitreous show a scleral route of distribution to the back of the eye. In the laser-induced CNV model in pigmented rabbits, topical ocular administration of SF0166 decreased lesion area compared with vehicle and was comparable to an injection of bevacizumab. In the VEGF-induced rabbit early neovascularization and vascular leakage model, topical ocular application of SF0166 resulted in a dose-dependent reduction in vascular leakage; the highest ocular doses tested showed comparable activity to an injection of bevacizumab. If comparable ocular concentrations can be achieved in humans after topical ocular administration, the concentration of SF0166 would be approximately 13,000-fold higher than the IC_{50} for inhibiting binding to $\alpha_v\beta_3$ and approximately 130-fold higher than the IC_{50} of SF0166 in the functional adhesion assay. If retention in retina and choroid in humans is comparable to that seen in rabbits (C_{last} = 751 ng/g at 12 hours), the SF0166 concentration would be >20-fold the IC_{50} in the functional assay.

JPET Fast Forward. Published on May 31, 2018 as DOI: 10.1124/jpet.118.248427
This article has not been copyedited and formatted. The final version may differ from this version.

Therefore, after administering an eye drop containing 2.5 mg SF0166, $\alpha_v\beta_3$ should be nearly completely inhibited for up to 12 hours.

SF0166 topical ophthalmic solution is intended to address limitations in current treatment of wet AMD and DME, which include agents requiring intravitreal injection every 4 to 12 weeks under local anesthesia. The activity of SF0166 in VEGF-driven models appears similar to that of anti-VEGF biologic drugs (e.g. bevacizumab). Moreover, SF0166 also blocks angiogenic signaling driven by other growth factors (FGF and PDGF [partially]), so clinical efficacy could exceed that of marketed drugs that only target VEGF.

SF0166 was efficacious in preclinical models of ocular neovascularization and vascular leakage and has completed nonclinical development, including safety pharmacology and toxicology studies required prior to testing in the clinic. SF0166 is currently being investigated in 2 clinical trials in patients with DME (NCT02914613) and AMD (NCT02914639). Both studies are Phase I/II, randomized, double-masked, multicenter clinical trials designed to evaluate the safety and exploratory efficacy after 28 days of SF0166 Topical Ophthalmic Solution BID and 28 days of post-treatment follow up.

ACKNOWLEDGEMENTS

Becky Norquist assisted with the preparation of this manuscript.

AUTHORSHIP CONTRIBUTIONS

Participated in research design: Askew, Furuya, Edwards

Conducted experiments: Askew

Performed data analysis: Askew

Wrote or contributed to the writing of the manuscript: Edwards

REFERENCES

Askew BC, Heidebrecht RW, Furuya T, and Duggan ME (2014) Fluorinated 3-(2-oxo-3-(3-arylpropyl)imidazolidin-1-yl)-3-arylpropanoic acid derivatives. US Patent US20140221410A1: SciFluor Life Sciences Inc.

Bourne RR, Stevens GA, White RA, Smith JL, Flaxman SR, Price H, Jonas JB, Keeffe J, Leasher J, Naidoo K, Pesudovs K, Resnikoff S, Taylor HR, and Vision Loss Expert Group (2013) Causes of vision loss worldwide, 1990-2010: a systematic analysis. *Lancet Glob Health* **1**: e339-349.

Congdon N, O'Colmain B, Klaver CC, Klein R, Muñoz B, Friedman DS, Kempen J, Taylor HR, Mitchell P, and Eye Diseases Prevalence Research Group (2004) Causes and prevalence of visual impairment among adults in the United States. *Arch Ophthalmol* **122**: 477-485.

Foster A and Resnikoff S (2005) The impact of Vision 2020 on global blindness. *Eye (Lond)* **19**: 1133-1135.

Gum GG, Wong CG, and de Carvalho RP (2005) Laser-induced models of choroidal neovascularization in rabbits associated with sustained suprachoroidal and episcleral delivery of VEGF and bFGF. *Invest Ophthalmol Vis Sci* **46**: 1422.

Henderson NC, Arnold TD, Katamura Y, Giacomini MM, Rodriguez JD, McCarty JH, Pellicoro A, Raschperger E, Betsholtz C, Ruminski PG, Griggs DW, Prinsen MJ, Maher JJ, Iredale JP, Lacy-Hulbert A, Adams RH, Sheppard D (2013) Targeting of αv integrin

identifies a core molecular pathway that regulates fibrosis in several organs. *Nat Med* **19**): 1617-1624.

Kupperman, BD. (2015) A dual-mechanism drug for vitreoretinal diseases. *Retina Today* **Jul/Aug**: 85-87.

Ludbrook SB, Barry ST, Delves CJ, and Horgan CM (2003) The integrin alphavbeta3 is a receptor for the latency-associated peptides of transforming growth factors beta1 and beta3. *Biochem J* **369**: 311-318.

Luna J, Tobe T, Mousa SA, Reilly TM, and Campochiaro PA (1996) Antagonists of integrin alpha(v)beta3 inhibit retinal neovascularization in a murine model. *Lab Invest* **75**: 563-573.

Murphy MG, Cerchio K, Stoch SA, Gottesdiener K, Wu M, Recker R; and L-000845704 Study Group (2005) Effect of L-000845704, an alphaVbeta3 integrin antagonist, on markers of bone turnover and bone mineral density in postmenopausal osteoporotic women. *J Clin Endocrinol Metab* **90**: 2022-2028.

Ponce ML and Kleinman HK (2003) Identification of redundant angiogenic sites in laminin alpha1 and gamma1 chains. *Exp Cell Res* **285**: 189-195.

Santulli RJ, Kinney WA, Ghosh S, Decorte BL, Liu L, Tuman RW, Zhou Z, Huebert N, Bursell SE, Clermont AC, Grant MB, Shaw LC, Mousa SA, Galemmo RA Jr, Johnson DL, Maryanoff BE, and Damiano BP (2008) Studies with an orally bioavailable alpha V integrin antagonist in animal models of ocular vasculopathy: retinal neovascularization

in mice and retinal vascular permeability in diabetic rats. *J Pharmacol Exp Ther* **324**: 894-901.

Silva RLE, Kanan Y, Mirando AC, Kim J, Shmueli RB, Lorenc VE, Fortmann SD, Sciamanna J, Pandey NB, Green JJ, Popel AS, and Campochiaro PA (2017) Tyrosine kinase blocking collagen IV-derived peptide suppresses ocular neovascularization and vascular leakage. *Sci Transl Med* **9**: pii:eaai8030.

Terai Y, Abe M, Miyamoto K, Koike M, Yamasaki M, Ueda M, Ueki M, and Sato Y (2001) Vascular smooth muscle cell growth-promoting factor/F-spondin inhibits angiogenesis via the blockade of integrin alphavbeta3 on vascular endothelial cells. *J Cell Physiol* **188**: 394-402.

Tsou R and Isik FF (2001) Integrin activation is required for VEGF and FGF receptor protein presence on human microvascular endothelial cells. *Mol Cell Biochem* **224**: 81-89.

Wilkinson-Berka JL, Jones D, Taylor G, Jaworski K, Kelly DJ, Ludbrook SB, Willette RN, Kumar S, and Gilbert RE (2006) SB-267268, a nonpeptidic antagonist of alpha(v)beta3 and alpha(v)beta5 integrins, reduces angiogenesis and VEGF expression in a mouse model of retinopathy of prematurity. *Invest Ophthalmol Vis Sci* **47**: 1600-1605.

Witmer AN, van Blijswijk BC, van Noorden CJ, Vrensen GF, Schlingemann RO (2004) In vivo angiogenic phenotype of endothelial cells and pericytes induced by vascular endothelial growth factor-A. *J Histochem Cytochem* **52**: 39-52.

FOOTNOTES

Funding: This work was supported by SciFluor Life Sciences, Inc.

Reprint requests:

D. Scott Edwards, Ph.D.

SciFluor Life Sciences

300 Technology Square

Cambridge, MA 02139, USA

E-mail: scott.edwards@scifluor.com

LEGENDS FOR FIGURES

Figure 1. Activity of SF0166 in CAM assay. **(A)** bFGF stimulation. **(B)** VEGF stimulation. **(C)** PDGF stimulation. Y-axis: blood vessels score. Staurosporine 1 µg was used as a positive control Error bars represent SEM. N = 5 per group. P-values for all treated groups were calculated by comparing with the vehicle group. *p<0.05, **p<0.01, ***p<0.001.

Figure 2. Mean (error bars represent SD) concentrations of SF0166 in plasma, aqueous humor, vitreous humor, and ocular tissues after a single ocular administration of 5% SF0166 to Dutch-Belted rabbits. N = 3 animals (6 eyes) per timepoint; mean of OD and OS combined. Units are ng/g for sclera and retina-choroid plexus and ng/mL for plasma, aqueous humor, and vitreous humor.

Figure 3. Mean (error bars represent SEM) neovascularization in the OIR mouse model. Mice were subjected to hyperoxia postnatal Days 7-12. On postnatal Days 13-17, mice received vehicle or 5% SF0166 BID. Retinal tissue was collected on postnatal Day 18. N = 7 animals (14 eyes) per group; OD and OS scores combined. Statistical analysis based on unpaired t-test.

Figure 4. Mean (error bars represent SD) CNV lesion area at specified timepoints (study days). **(A)** Right eye (OD). **(B)** Left eye (OS). CNV was induced by laser treatment on Day -3. Lesion area measurements were performed on Day 0; dosing started on Day 1 (2.5% BID SF0166; single injection of 1.25 mg/eye bevacizumab). N =

24 lesions per group (4 lesions per eye, 3 animals per group). Post-dose lesion area measurements were made weekly starting on Day 4. Statistical analysis based on ANOVA with Dunnett's multiple comparison test *p<0.05, **p< 0.01, ***p< 0.001 (all comparisons to vehicle group). The same lesions (4/eye) were tracked throughout study.

Figure 5. Mean (error bars represent SD) vascular leakage measured by fluorescein angiography. Vascular leakage was induced on Day 3 via intravitreal injection of VEGF (2 days after the start of study drug dosing on Day 1). Fluorescein imaging was performed after 8 days of dosing (Day 8) with the indicated concentrations of SF0166. N = 6 animals (12 eyes) per group; OD and OS scores combined.

TABLES

Table 1. Activity of SF0166 and L-000845704 in blocking cell adhesion to vitronectin (vn) and fibronectin (fn)

	K562		HT29		HMVEC		RLMVEC	
	vn	fn	vn	fn	vn	fn	vn	fn
Compound	IC_{50}, μM	IC_{50}, μM	IC_{50}, μM	IC_{50}, μM	IC_{50}, μM	IC_{50}, μM	IC_{50}, μM	IC_{50}, μM
SF0166	0.00161	3.04	0.00129	0.00127	0.00105	159	0.00000761	930
L-000845704	0.00118	1.81	0.00159	0.00533	0.00110	46.3	0.0000286	239

N = 2-4 per group.

JPET Fast Forward. Published on May 31, 2018 as DOI: 10.1124/jpet.118.248427
This article has not been copyedited and formatted. The final version may differ from this version.

Table 2. Ocular tissue pharmacokinetic parameters after a single ocular administration of 5% SF0166 (2.5 mg/eye) to Dutch-Belted rabbits

Sample	C_{max} (ng/mL or ng/g)	T_{max} (hr)	C_{last} (ng/mL or ng/g)	T_{last} (hr)	$AUC_{0\text{-}last}$ (hr·ng/mL or hr·ng/g)
Aqueous humor	2033 (720)	1 (1, 1)	12.0 (3.19)	12 (12, 12)	5126 (1550)
Vitreous humor	352 (334)	1 (1, 4)	52.3 (47.0)	12 (12, 12)	1298 (986)
Sclera	9417 (6156)	1 (1, 1)	1845 (1394)	12 (12, 12)	45699 (33078)
Retina-choroid plexus	5103 (4368)	1 (1, 8)	751 (506)	12 (12, 12)	24395 (17534)

Values are mean (SD), except for T_{max} and T_{last}, which are median (range). Values are mean of OD and OS combined. N = 12 animals (6 eyes per timepoint). Units are ng/mL for aqueous and vitreous humors and ng/g for sclera and retina-choroid plexus.

FIGURES

JPET Fast Forward. Published on May 31, 2018 as DOI: 10.1124/jpet.118.248427
This article has not been copyedited and formatted. The final version may differ from this version.

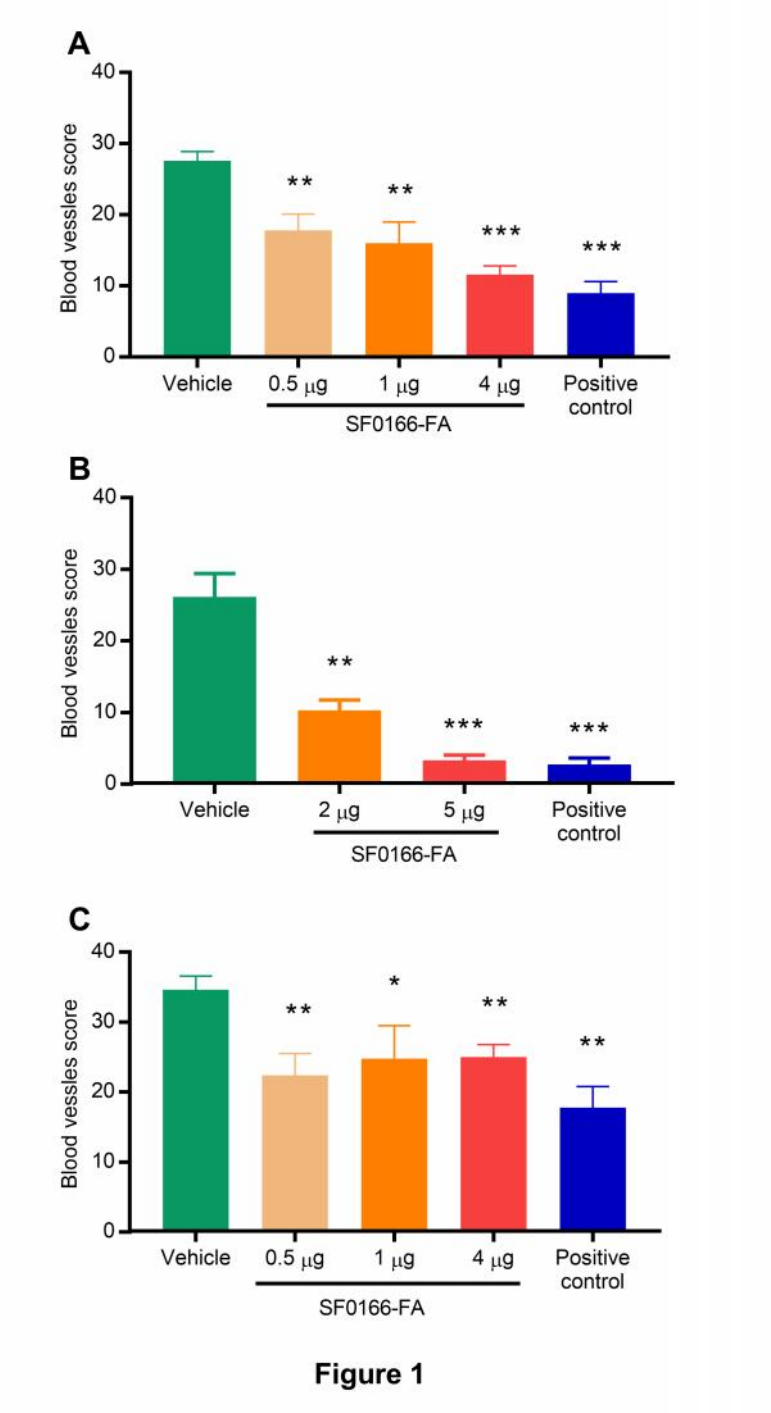

Figure 1

JPET Fast Forward. Published on May 31, 2018 as DOI: 10.1124/jpet.118.248427
This article has not been copyedited and formatted. The final version may differ from this version.

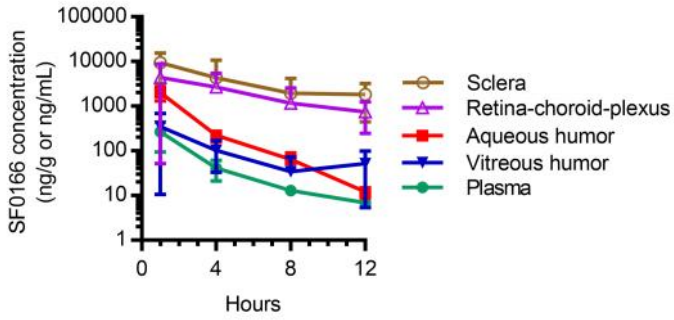

Figure 2

JPET Fast Forward. Published on May 31, 2018 as DOI: 10.1124/jpet.118.248427
This article has not been copyedited and formatted. The final version may differ from this version.

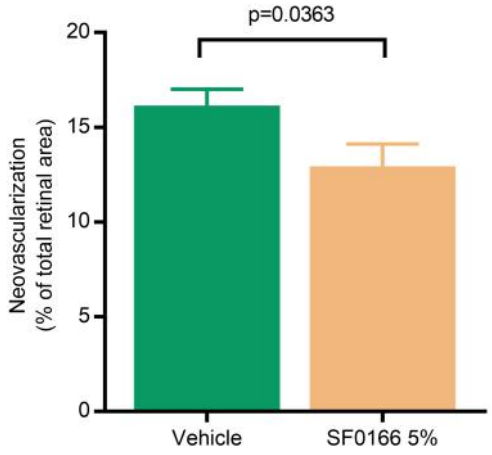

Figure 3

JPET Fast Forward. Published on May 31, 2018 as DOI: 10.1124/jpet.118.248427
This article has not been copyedited and formatted. The final version may differ from this version.

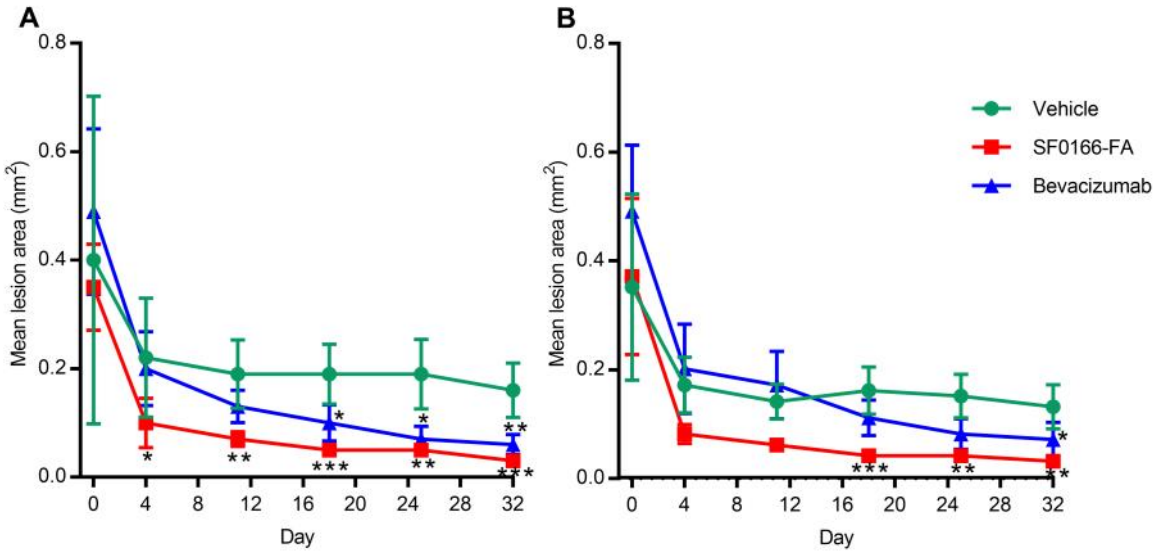

Figure 4

JPET Fast Forward. Published on May 31, 2018 as DOI: 10.1124/jpet.118.248427
This article has not been copyedited and formatted. The final version may differ from this version.

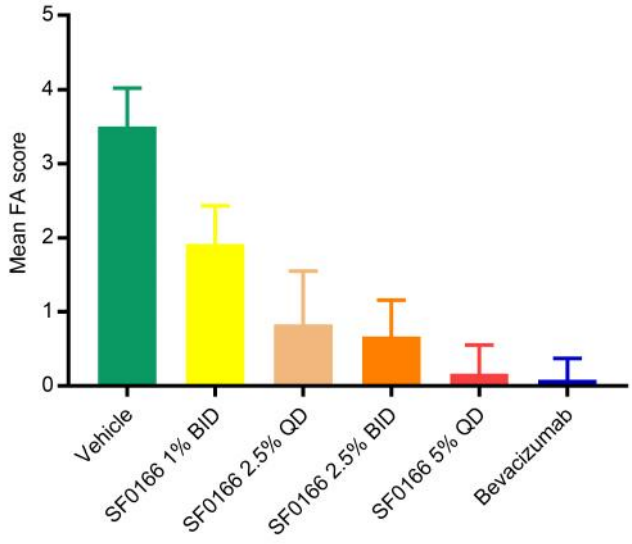

Figure 5

Supplementary Materials

Journal of Pharmacology and Experimental Therapeutics

Ocular Distribution and Pharmacodynamics of SF0166, a Topically Administered $\alpha_v\beta_3$ Integrin Antagonist, for the Treatment of Retinal Diseases

Ben C. Askew, Takeru Furuya, and D. Scott Edwards

Supplementary Table 1. Scoring scale for the laser-induced CNV model study in Dutch-Belted rabbits

Score	Description
Conjunctival Discharge	
0	Normal. No discharge.
1	Discharge above normal and present on the inner portion of the eye but not on the lids or hairs of the eyelids.
2	Discharge is abundant, easily observed and has collected on the lids and hairs of the eyelids.
3	Discharge has been flowing over the eyelids so as to wet the hairs substantially on the skin around the eye.
Conjunctival Congestion	
0	Normal. May appear blanched to reddish pink without perilimbal injection (except at the 12:00 and 6:00 positions) with vessels of the palpebral and bulbar conjunctiva easily observed.
1	A flushed, reddish color predominantly confined to the palpebral conjunctiva with some perilimbal injection but primarily confined to the lower and upper parts of the eye from the 4:00 to 7:00 and 11:00 to 1:00 positions.
2	Bright red color of the palpebral conjunctiva with accompanying perilimbal injection covering at least 75% of the circumference of the perilimbal region.
3	Dark, beefy red color with congestion of both the bulbar and palpebral conjunctiva along with pronounced perilimbal injection and the presence of petechia on the conjunctiva. The petechia generally predominates along the nictitating membrane and upper palpebral conjunctiva.
Conjunctival Swelling	
0	Normal or no swelling of the conjunctival tissue
1	Swelling above normal without eversion of the eyelids (easily discerned by noting upper and lower eyelids are positioned as in the normal eye); swelling generally starts in the lower cul-de-sac near the inner canthus.
2	Swelling with misalignment of the normal approximation of the lower and upper eyelids; primarily confined to the upper eyelid so that in the initial stages, the misapproximation of the eyelids begins by partial eversion of the upper eyelid. In this stage the swelling is confined generally to the upper eyelid with some swelling in the lower cul-de-sac.
3	Swelling definite with partial eversion of the upper and lower eyelids essentially equivalent. This can be easily observed by looking at the animal head-on and noting the position of the eyelids; if the eye margins do not meet, eversion has occurred.
4	Eversion of the upper eyelid is pronounced with less pronounced eversion of the lower eyelid. It is difficult to retract the lids and observe the perilimbal region.

Iris Involvement	
0	Normal iris without any hyperemia of the blood vessels.
1	Minimal injection of the secondary vessels but not tertiary vessels. Generally uniform but may be of greater intensity at the 12:00 to 1:00 or 6:00 position. If confined to this area, the tertiary vessels must be substantially hyperemic.
2	Minimal injection of tertiary vessels and minimal to moderate injection of the secondary vessels.
3	Moderate injection of the secondary and tertiary vessels with slight swelling of the iris stroma (the iris surface appears slightly rugose, usually most predominant near the 3:00 and 9:00 positions).
4	Marked injection of the secondary and tertiary vessels with marked swelling of the iris stroma. The iris appears rugose; may be accompanied by hemorrhage (hyphema) in the anterior chamber.
Cornea	
0	Normal cornea.
1	Some loss of transparency. Only the epithelium and/or the anterior half of the stroma are involved. The underlying structures are clearly visible although some cloudiness may be readily apparent.
2	Involvement of the entire thickness of the stroma. With diffuse illumination, the underlying structures are just barely visible (can still observe flare, iris, pupil response, and lens).
3	Involvement of the entire thickness of the stroma. With diffuse illumination, the underlying structures cannot be seen.
Surface Area of Cornea Involvement	
0	Normal.
1	1-25% area of stromal cloudiness.
2	26-50% area of stromal cloudiness.
3	51-75% area of stromal cloudiness.
4	76-100% area of stromal cloudiness.
Pannus	
0	No pannus (vascularization of the cornea).
1	Vascularization present but vessels have not invaded the entire cornea circumference.
2	Vessels have invaded 2 mm or more around entire corneal surface.
Pupillary Response	
0	Normal pupil response.
1	Sluggish or incomplete pupil response.
2	No pupil response.
3	No pupil response due to pharmacological blockage.

Aqueous Flare	
0	None
1	1+
2	2+
3	3+
4	4+ (fibrin)
Cellular Flare	
0	None
1	1+
2	2+
3	3+
4	4+
Lens	
0	Lens clear.
1	Anterior (cortical/capsular).
2	Nuclear.
3	Posterior (cortical/optical).
4	Equatorial.
Vitreous	
0	Clear vitreous.
1	Few scattered opacities, fundus unimpaired.
2	Moderate scattered opacities, fundus details somewhat obscured.
3	Many opacities, marked blurring of fundus details.
4	Dense opacities, no fundus view.
Vitreal Hemorrhage	
0	None
1	1-25%
2	26-50%
3	51-75%
4	76-100%

Retinal Detachment	
0	None.
1	Rhegmatogenous (retinal detachment occurs when subretinal fluid accumulates in the potential space between the neurosensory retina and the underlying retinal pigment epithelium).
2	Exudative (occurs due to inflammation, injury, or vascular abnormalities that results in fluid accumulating underneath the retina without the presence of a hole, tear, or break).
3	Tractional (occurs when fibrous or fibrovascular tissue, caused by an injury, inflammation, or neovascularization that pulls the sensory retina from the retinal pigment epithelium).
Retinal Hemorrhage	
0	None
1	1-25%
2	26-50%
3	51-75%
4	76-100%
Choroidal/Retinal Inflammation	
0	None
1	Mild
2	Moderate
3	Severe

Supplementary Table 2. Scoring scale used to determine fluorescein angiography score for the VEGF-induced vascular leakage study in Dutch-Belted rabbits

Score	Description
0	Major vessels straight some tortuosity of smaller vessels, no vessel dilation
1	Increased tortuosity of major vessels and/or some vessel dilation
2	Leakage between major vessels, significant vessel dilation
3	Leakage between major and minor vessels, minor vessels still visible
4	Leakage between major and minor vessels, minor vessels poorly/not visible

Supplementary Table 3. Design for the VEGF-induced vascular leakage study in Dutch-Belted rabbits

Test Article	Dosing	Dose (mg/eye)	Dose Concentration (%)	Dose Volume (µL/eye)
SF0166	Ocular (Topical, OU, QD starting Day 1)	2.5	5	50
SF0166	Ocular (Topical, OU, BID starting Day 1)	1.25	2.5	50
SF0166	Ocular (Topical, OU, QD starting Day 1)	1.25	2.5	50
SF0166	Ocular (Topical, OU, BID starting Day 1)	0.5	1.0	50
Vehicle	Ocular (Topical, OU, QD starting Day 1)	—	—	50
Bevacizumab	Ocular (IVT, OU, single administration on Day 1)	1.25	2.5	50

BID: twice daily; IVT: intravitreal; OU: both eyes; QD: once daily

Animals were dosed with test article starting Day 1. VEGF was injected on Day 3. N = 6 per group.

Vehicle

Baseline score = 0 Day 8 score = 4

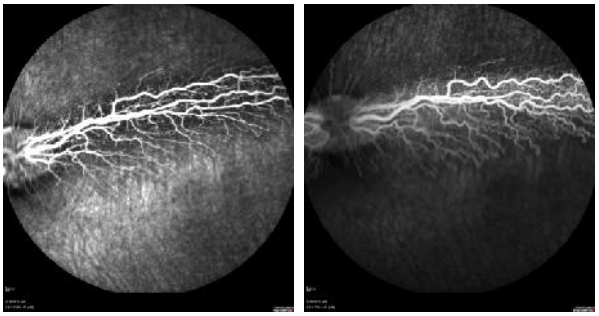

SF0166 1% BID

Baseline score = 0 Day 8 score = 2

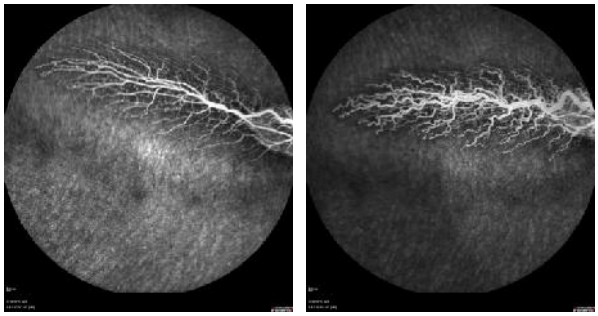

SF0166, 2.5% QD

Baseline score = 0 Day 8 score = 1

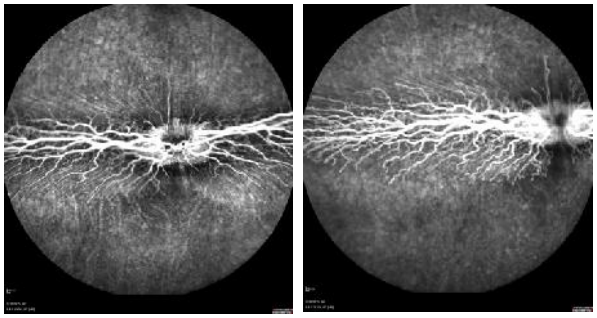

SF0166, 2.5% BID

Baseline score = 0 Day 8 score = 1

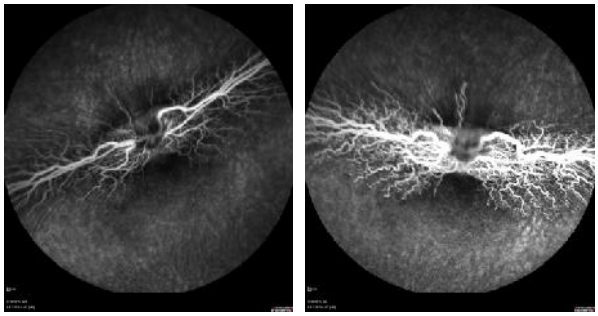

SF0166, 5% QD

Baseline score = 0 Day 8 score = 0

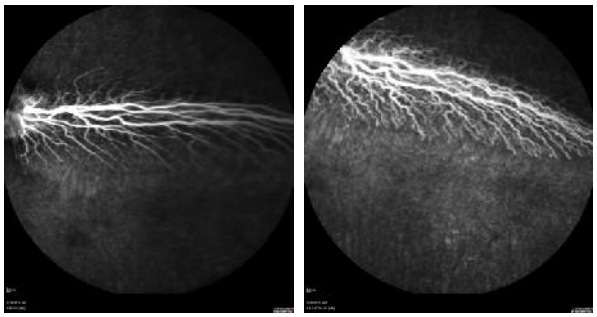

Bevacizumab

Baseline score = 0 Day 8 score = 0

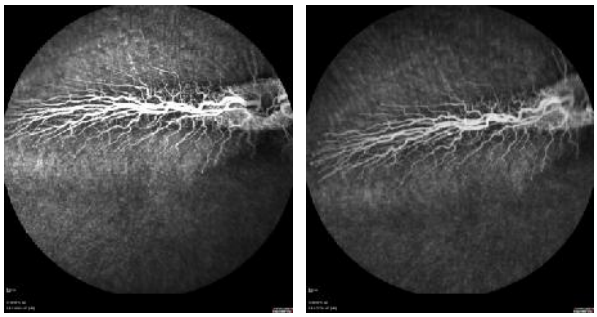

Supplementary Figure 1. Representative fluorescein images from the VEGF-induced vascular leakage study in Dutch-Belted rabbits. Images were taken at baseline and Day 8.